Ingénierie des Systèmes d'Information
Vol. 27, No. 6, December, 2022, pp. 875-885
Journal homepage: http://iieta.org/journals/isi

Fairness Oriented H-NOMA Devices Association and Pairing in HCN Slicing Using Cooperation Games

Mai A. Riad[1*], Osama M. El-Ghandour[1,2], Ahmed M. Abd El-Haleem[1]

[1] Electronics and Communications Engineering Department, Faculty of Engineering, Helwan University, Cairo 11795, Egypt
[2] Electronics and Communications Engineering Department, Higher Institute for Engineering, Institute Undersecretary for Education and Student Affairs, Fifth Settlement, Cairo 4722501, Egypt

Corresponding Author Email: mai_awad_reyad@h-eng.helwan.edu.eg

https://doi.org/10.18280/isi.270603

Received: 26 September 2022
Accepted: 20 December 2022

Keywords:
5G, RAN slicing, HCN, eMBB, uRLLC, H-NOMA, NBS, matching game

ABSTRACT

Device association (DA) and pairing (DP) are presented in this letter to evaluate the fairness of different services between enhanced mobile broadband devices (eMBBDs) and ultra-reliability low latency communications devices (uRLLCDs) in RAN-slicing, which has emerged as a viable technique for enhancing total network throughput in heterogeneous cellular networks (HCNs) design. To optimize the eMBBDs' downlink (DL) sum rate while fulfilling the provisions of the uRLLC traffic. A cooperative Nash bargaining solution (NBS) is formulated to depict the association method. First, base stations (BSs) create random pairings between heterogeneous non-orthogonal multi-access (H-NOMA) devices. The BSs are classified into coalitions through the Hungarian approach. So, a two-band partition algorithm is evolved for the two BSs in each coalition to negotiate their allocated devices to improve the NBS utility. A multiplayer bargaining approach is constructed using this algorithm and the Hungarian technique. After finishing the DA process, we study the cooperative matching algorithm to optimize the pairing problem between devices' slices. Simulation results demonstrate that comparing the proposed approach to other schemes can achieve a significant DL rate distribution for eMBBDs, device-side latency for uRLLCDs, and fairness improvements.

1. INTRODUCTION

In recent years, the exponential rise of mobile telecommunication, smart devices, and traffic request have necessitated the optimization of cellular concentration to enable high data rate and less delay in vast networks [1, 2]. Reutilizing the spectrum between HCN base stations is one of the most efficient methods. Where HCN increases system capacity and energy efficiency by using a more flexible design for transmission power distribution and using PBS with a more compact and dense coverage area. Connecting devices to several HCN BSs is a significant challenge in HCNs [3]. To face the massive connectivity problem, some methods have been proposed in the past few years to replace the traditional orthogonal multiple access (OMA). NOMA can boost devices more than the number of obtainable resources [4], guiding to more spectral effectiveness and device justice than criterion OMA approaches. The precept of NOMA benefits the idea of superposition coding (SPC) at the sender to collect devices in the power domain and successive interference cancellation (SIC) at the recipient [5]. The International Telecommunications Union (ITU) has categorized service needs into three categories [6]: Massive Machine Type Communication (mMTC) enhanced Mobile Broadband (eMBB), and ultra-Reliable and Low-Latency Communications (uRLLC). eMBB focuses on services with high bandwidth requirements, mMTC on services with high communication density demands, and uRLLC on services sensitive to latency. However, these services can only be deployed via a shared network strategy. Optimizing the network, for instance, for low latency, Hybrid Automatic Repeat reQuest (HARQ) retransmissions, and high dependability may result in a spectral efficiency trade-off [7]. In this context, network slicing (NS) has protruded as a crucial facilitator for upgrading 5G networks via multiple services [8]. The primary advantage of NS [9] is operating many conceptually separated networks as independent business activities atop a shared physical infrastructure.

In everyday life, a market serves as a focal collecting place where individuals may trade items and negotiate deals to their satisfaction. Game theory was chosen so that users and BSs can work together to share some information and get better payoffs. Players may bargain with each other to decide how to share information if there is such extra utility if they cooperate. Similarly, NS may act as a market function in multiuser and HCN H-NOMA systems. The spread BSs can negotiate, through the network, to collaborate in making choices about the connected users so that each may function at its optimal level and mutual agreements are formed over their operating points based on NBS. A matching game was also designed to efficiently deploy coordinated multi-point transmissions through cooperation among the network's users. Consequently, the newly formed slice serves as a customized network for a particular service. The network slice may incorporate core network (CN) and radio access network (RAN) components to meet end-to-end service requirements. However, establishing uRLLC is still challenging [10]. On account of finite capacity, radio channels, and execution segregation, RAN slicing

presents additional challenges and is still in its infancy. This study aims to tackle the user-association and pairing problems in 5G HCN by presenting a unique RAN slicing architecture capable of decreasing interference, supporting the diverse QoS requirements of users, and enhancing overall network performance.

2. RELATED WORK

Wireless networks segment infrastructure to save money and maximise spectrum use. From problems of NS in HetNet that includes user association and resource allocation. Also, most research has seen NS's chains-isolated resource distribution as an important matter, RAN slicing realizes Earliest Deadline First (EDF) scheduling utilized in actual-time operative systems to allocate resources [11]. And [12] a communication-theoretic model was constructed for orthogonal and non-orthogonal slicing for eMBB, mMTC, and uRLLC uplink services. Non-orthogonal slicing may improve performance for all services by exploiting their different demands. NOMA is a prime option for 5G networks which enjoy high spectrum competence (eMBB), user Connection (mMTC), and less delay (uRLLC) [13]. The rate-splitting multiple access (RSMA) is employed for uRLLC transport, where a uRLLC user breaks its packet into two sub-messages based on the mean signal-to-noise ratio (SNR) without instant channel status information (CSI) [14]. uRLLC and eMBB coexistence in MIMO NOMA systems are investigated using puncturing [15]. This research [16] analyses uRLLC and eMBB coexistence in a cell network with a reconfigurable intelligent surface (RIS). eMBB clients use enhanced Pre-emptive Scheduling (EPS) scheduler for downlink ergodic capacity [17]. uRLLC and eMBB connections have been encrypted in the cloud and decrypted at brim nodes to achieve delay limitations [18]. [19] is proposed eMBB transport danger and uRLLC confidence as risk indicators for eMBB transport to provide adjuster, proportional resource distribution to coming uRLLC load. uRLLC scheduling is depended on Deep Reinforcement Learning (DRL) to boost eMBB throughput [20]. This study employs linear, convex, and threshold eMBB rate loss to distribute uRLLC traffic [21]. The Nobel Prize-winning matching game framework has lately been recognized as a viable wireless resource allocation, user association, and user pairing method [22]. User association in cellular virtualization networks has been modeled as a matching game that considers users' preferences, QoS requirements, and backhaul constaints [23]. The authors have wanted to boost the eMBB network throughput and cut down on eMBB lack by getting uRLLC users and eMBB users to work together by using a superposition predisposition game theory [24]. Matching game algorithms for user connection in HCNs that consider both uplink and downlink features have been shown [25]. A method called "puncturing" has been used to increase the number of eMBB users by using a one-sided matching game to stop eMBB and uRLLC from being scheduled simultaneously [26]. The matching theory has been used to disband the problem of matching users and allocating power in the cognitive radio non-orthogonal multiple access (CR-NOMA) systems [27]. Utilizing a homogeneous NOMA per slice in downlink and uplink with justice boosts the network rate for all devices [28]. Multi-Connectivity (MC)-BSa increase resources and minimise wait times by sharing spectrum among base stations and delivering differentiated QoS for rate and machine-to-machine (M2M) services. On the other hand, few authors concentrate on users' associations of the diverse services with BSs [29]. This effort aims to provide 5G's isolation and springiness by solving the user connection [30]. The Pointer Network (PtrNet) architecture supports NOMA's user association and pairing [31]. Whilst, none of those aforementioned above addresses intra and inter-isolation overlaps between slices when analysing cell association or resource allocation addresses intra and inter-isolation overlap between slices when analysing cell connection or resource allocation. Also, previous research projects separately focused on resource allocation or user association in different NS. This letter proposes new device association and pairing algorithms in a downlink two-tier HCN for coexisting eMBBDs and uRLLCDs that consider each device type's diverse association and pairing requirements. The device association problem is formulated as a cooperative bargaining game problem, where different devices compete on the available data streams across all BSs. The Nash Bargaining Solution (NBS) criterion provides a unique and fair solution for the formulated bargaining problem. And then, a matching-game theoretic approach for the device-slice pairing problem is suggested to provide the total of the DL throughput and fulfilling the provisions of the uRLLC traffic.

3. SYSTEM MODEL

Consider a two-tier downlink H-NOMA cellular network with a single infrastructure provider (InP). The first tier is modelled as macrocell, while the second tier is modelled as picocells, as shown in Figure 1. The set of BSs is denoted as β, including MBS and PBSs where $b = 1$ refers to MBS, $b = 2,3, \ldots, \beta$ implies pico-cells covered by MBS. All BSs share the same bandwidth. Let D^{eMBB} and D^{uRLLC} denote a set of eMBBDs and uRLLCDs, respectively. Then, Then, the devices' set is indicated by $D = D^{eMBB} \cup D^{uRLLC}$ with cardinality $\mathcal{D}$. InP provides infrastructure services to several mobile virtual network operators (MVNOs). Virtual resources are sliced and assigned to serve devices into two different network slices $s \in S = \{1, 2\}$, i.e., for eMBB and uRLLC. Each slice s owns a group of devices indicated by I_s, let $i = \cup_{s=1}^{S} I_s$ where $|\cdot|$ is the cardinality of the set of all devices. The set of uRLLCDs and eMBBDs by $l = \{1, 2, 3, \ldots\} \in D^{uRLLC}$ and $e = \{1, 2, 3, \ldots\} \in D^{eMBB}$, respectively are at random dispensed through the whole network region. Each resource block (RB) can particularly serve two diverse service devices when H-NOMA is employed. Implementing H-NOMA brings more complicated co-channel interferences (CCI) to the current systems; to limit the major trouble without CCI using ideal SIC, the superimposed signal is received by both uRLLCD and eMBBD, and each device applies SIC to decipher its data [32]. The stronger device is supposed as a uRLLCD that only can decipher and remove CCI from the low device is eMBBD. Whilst the eMBBD with the weakest channel conditions couldnot wholly cancel the interference of uRLLCDs' messages, which results in increased rate for the eMBBD. With β base stations, each with $\mathcal{N}$ RBs, the network may support $2\beta\mathcal{N}$ devices concurrently utilizing H-NOMA [31]. We assume a system design in which eMBB traffic is transmitted over long TTIs $\mathcal{T}$, while uRLLC traffic is transmitted over short TTIs δ by superimposing the ongoing eMBB transmissions [20]. Here, transmitting the incoming uRLLC traffic in the short TTI ensures its latency requirement.

The data rate of eMBB traffic is captured by Shannon's capacity considering the impact of uRLLC transmissions, while uRLLC depends on the finite block-length capacity model due to its small packet size nature [20]. TDMA in each time slot; $\mathcal{Q}\ D^{uRLLC}$ couple with D^{eMBB} at different mini-slots. We first begin by figuring out the binary association matrix $\boldsymbol{\mathcal{A}}$ to reproduce the device association issue, in which a_{db} is an element of $\boldsymbol{\mathcal{A}}\ \forall\ d \in D, b \in \beta$. Likewise, where a_{db}= 1 when device d is associated with BS b, 0 otherwise. Second, we figure out the binary pairing matrix $\mathcal{X}$ to reproduce the device pairing issue, in which x_{db} is an element of $\mathcal{X}\ \forall\ d \in D, b \in \beta$. Likewise, where x_{le}= 1 when the associated devices l *and* e are paired in the same BS b, 0 otherwise.

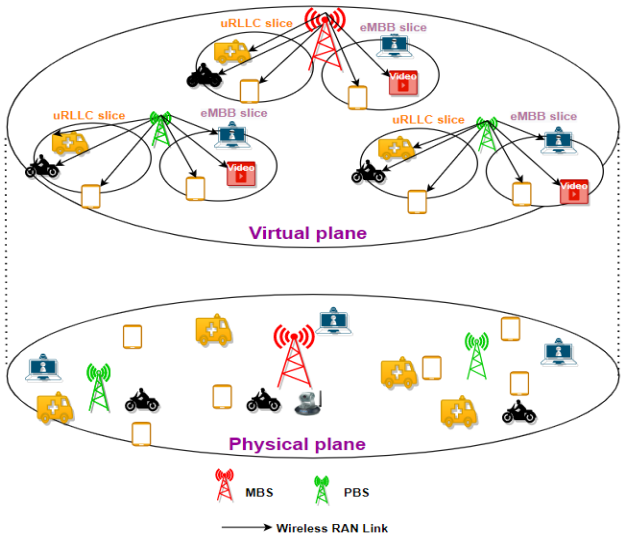

Figure 1. Two-tier HCN with eMBB/uRLLC slices of devices co-existence

eMBB Slice: We consider the DL signal-to-interference and noise ratio (SINR) is received by the eMBBD $e \in D^{eMBB}$ from BS $b \in \beta$ is given by

$$\Gamma_{eb} = \frac{(1-\varrho_b)\, P_b\, \hbar_{eb}}{\varrho_b\, P_b\, \hbar_{eb} + \sum_{k \neq B \setminus \{b\}} (1-\varrho_k)\, P_k\, \hbar_{ek} + \sigma^2} \tag{1}$$

where, P_b represents the transmitted power from BS b, $\hbar_{eb}$ indicates the BS-to-device e average channel gain, $(1-\varrho_b) \in [0, 1]$ denotes the power allocation coefficient for the eMBBD associated with $b \in \beta$ by a device e; and σ^2 represents additive noise power.

uRLLC Slice: Similarly, the DL signal-to-interference and noise ratio (SINR) is received by the uRLLCD $l \in D^{uRLLC}$ from BS $b \in \beta$ is given by

$$\Gamma_{lb}^{m} = \frac{\varrho_b\ P_b\ \mathcal{G}_{lb}}{\sum_{k \neq B \setminus \{b\}} (1-\varrho_k)\ P_k\ \mathcal{G}_{lk}\ +\ \sigma^2} \tag{2}$$

where, $\varrho_b \in [0, 1]$ denotes the power allocation coefficient for the uRLLCD associated with $b \in \beta$ and device l, $\mathcal{G}_{lb}$ represents the BS-to-device$l$ average channel gain.

The effective load of BS $b \in \beta$ is defined as the number of associated devices with it, i.e., $\sum_{d \epsilon D} a_{db}$. The resources' fraction used by each BS-connected device is $1/\sum_{d \epsilon D} a_{db}$ [33]. Then, the associated devices e and l with BS b data rates are provided below

$$r_{eb} = \left(\sum_{e \epsilon D^{eMBB}} a_{eb}\right)^{-1} \mathcal{W} \log_2(1 + \Gamma_{eb}) \tag{3}$$

$$r_{lb} = \left(\sum_{l \epsilon D^{uRLLC}} a_{lb}\right)^{-1} \mathcal{W} \log_2(1 + \Gamma_{lb}^{m}) - \sqrt{\frac{V_{lb}}{\mathcal{C}_{lb}}}\, Q^{-1}(\varepsilon) \tag{4}$$

where, $\mathcal{W}$ denotes the operational frequency bandwidth of the system, $\mathcal{C}_{lb}$ is the block-length code, and Q is the complementary Gaussian cumulative distribution function with the probability of decoding error $\boldsymbol{\varepsilon}$ and V_{lb} is the channel dispersion where is symbolized by $V_{lb} = 1 - \frac{1}{(1-\Gamma_{lb})^2}$. For providing inter-slice isolation and QoS for every device-slice following H-NOMA technique, we suppose $\mathcal{R}_{sb}^{rsv}$ as the threshold rate for every slice in the BS [34, 35]. We give the eMBB slice the $\mathcal{R}_{1b}^{rsv}$ rate and the uRLLC slice the $\mathcal{R}_{2b}^{rsv}$ rate. The overall rate of the cell is indicated as $\mathcal{R}_{b}^{rsv}$=$\mathcal{R}_{1b}^{rsv} + \mathcal{R}_{2b}^{rsv}$; depending on the mean DL physical rate of LTE system is implemented by [36].

4. PROPOSED NBS BASED DEVICE ASSOCIATION

4.1 Problem formulation

This subsection analyses device association as a Nash bargaining game including cooperation, [37] showing how to do this. In this example, let's say that $\mathcal{B} = \{1, 2, \ldots b, \ldots, \beta\}$ is the set of players that are the BSs. Let $U = (U_1, \ldots, U_b, \ldots, U_{\mathcal{B}})$ is a convex and closed subset of $\Re^{\mathcal{B}}$. That can figure out the possible payoff allocation set for each player if they all work together. We can think of the minimum performance of each player b as U^{min}= $(U_1^{min}, \ldots, U_b^{min}, \ldots, U_{\mathcal{B}}^{min})$. To ensure that the player gets paid, $U_b \in U \setminus U_b \geq U_b^{min}\ \forall\ b \in \mathcal{B}$ isn't a set with no empty spaces. Then, the pair (U, U^{min}) comes up with a problem for a $\mathcal{B}$-person to solve. Because of this, the $\mathcal{B}$-person bargaining problem's solution, is called as NBS [33], Thus, the joint optimization problem of device association can be represented as a NBS game, i.e.

$$U^{*} = \arg\max_{A} \prod_{b=1}^{\mathcal{B}} (U_b - U_b^{min}) \quad S.t.\ U_b \geq U_b^{min} \tag{5}$$

Let us now define a fair device association for BSs: A fair device association among BSs simplifies the BSs' backhaul architecture and ensures that all devices are treated equitably. According to [33, 38-40], an optimum and unique NBS if U_b is a concave function with convex support that is upper-bounded. Provided that BSs are portrayed as players in this context, the reward of each BS $b \in \mathcal{B}$ may be designated as the total utility of all devices connected with it, as specified by

$$U_b = \sum_{e \epsilon D^{eMBB}} a_{eb}\ \varphi_{eb} + \sum_{l \epsilon D^{uRLLC}} a_{lb}\ \varphi_{lb} \tag{6}$$

According to that, the different association metrics are used to reflect the properties of each device type; eMBBDs and uRLLCDs. The combined DL rate is used as association measures for eMBBDs and uRLLCDs. Additionally, the proportional fairness criteria are used as described in [40] to ensure justice among devices. Therefore, the utility of the devices $e \in D^{eMBB}$ and $l \in D^{uRLLC}$ when used in combination with BS $b \in \mathcal{B}$ may be described as follows:

$$\varphi_{eb} = \log\left(r_{eb}/r_{eb}^{min}\right), \quad \forall\, e \in D^{eMBB} \tag{7}$$

$$\varphi_{lb} = \log(r_{lb}/r_{lb}^{min}), \quad \forall\, l \in D^{uRLLC} \tag{8}$$

Thus, the payment for each BS will thus be as follows:

$$\begin{aligned} U_b = & \sum_{e \in D^{eMBB}} a_{eb}\ \log(r_{eb}/r_{eb}^{min}) + \\ & \sum_{l \in D^{uRLLC}} a_{lb}\ \log\left(r_{lb}/r_{lb}^{min}\right) \\ & = \sum_{d\ \in\ D} a_{db}\ \log(r_{db}/r_{db}^{min}) \end{aligned} \tag{9}$$

Thus, the device association optimization problem is represented as

$$OP\ T1\ -DA: \max_{A} U\ = \prod_{b=1}^{\mathcal{B}} (U_b - U_b^{min}) \tag{10}$$

$$\text{S.t} \qquad U_b\ \geq U_b^{min}, \qquad \forall\, b \in \mathcal{B} \tag{10a}$$

$$a_{db} \in \{0,1\}, \qquad \forall\, d \in D,\ b \in \mathcal{B} \tag{10b}$$

$$\sum_{b \in \mathcal{B}} a_{db} = 1 \qquad \forall\, d \in D,\ = D^{eMBB} \cup D^{uRLLC} \tag{10c}$$

where, U is the NBS utility and U_b^{min} denotes the BS b minimum revenue, which is set to zero in the absence of any linked devices. The restriction in (10c) describes the association constraint which each device i_s can connect with a single BS. The optimization objective is to identify $\mathcal{A}$ that maximizing all U_b simultaneously.

4.2 Bargaining algorithm for Two-BS case

This part has explained the scenario when $\mathcal{B} = 2$ and develops a two-BS bargaining method. The concept behind solving the two-BS bargaining issue is to allow two BSs to negotiate and swap their connected devices to achieve mutual benefit. Inspired by the low complexity algorithm [41], the so-called two-band partition is applied to determine the opportunistic user association. It is shown [41] that the two-band partition is near-optimal for the optimization goal of weighted rate maximization.

At the start-up stage, we correlate devices with the BS to improve SINR during setup. This increases our possibility of reaching the NBS by boosting our Nash product before bargaining. MBS transmits with more power. Two situations result in unfair initialization. MBSs can be started with many devices, whereas PBSs can't. Second, MBS may not have as many devices as PBSs, while having a greater data rate, utility, and Nash production before bargaining. To ensure equitable initialization, we define" initial effective load" as the maximum number of devices associated with each BS during start-up. As for devices, we use [42], for MBS and PBS to get a larger Nash product before bargaining. uRLLC initialization load should not exceed $\mathcal{Q}$, where $\mathcal{Q}$ is the number of uRLLCD/eMBBD pairs per time slot. Assume random pairing between uRLLCDs and eMBBDs, the device association is determined using the two-band partition technique [41], as demonstrated in Table 1. The optimization objective in our model is to maximize the NBS function $U = (U_1 - U_1^{min})(U_2 - U_2^{min})$. Similarly [37]; limitation (10b) is relaxed to allow for continuous values when $0 \leqslant a_{i_s b} \leqslant 1$ is used. Let $\mu = \mu_d$, $d \in D$ equal to the Lagrange multiplier vector. Then, the Lagrangian role of (10) may be represented by the following role of $a_{i_s b}$:

$$L = \prod_{b=1}^{2} (U_b - U_b^{min}) + \sum_{d \in D} \mu_d \left(\sum_{b=1}^{2} a_{db} - 1 \right) \tag{11}$$

By applying Karush-Kuhn-Tucker (KKT) constraints to (11) and taking the derivative regarding a_{db}

$$\frac{\varphi_{d1} - 1}{U_1 - U_1^{min}} = \frac{\varphi_{d2} - 1}{U_2 - U_2^{min}} \tag{12}$$

The marginal advantages of device *e* for the two BSs (BS1 and BS2) are clarified on the left-hand side (LHS) and right-hand side (RHS) of (12). If the *e* device is connected to BS1, the RHS of (12) should be lower than the LHS, and vice versa for BS2. Observe the relationship between LHS and RHS as a function in φ_{d1}, φ_{d2}, and write it as $f(\varphi_{d1}, \varphi_{d2})$ as follows

$$f(\varphi_{d1}, \varphi_{d2}) = \frac{\varphi_{d1} - 1}{U_1 - U_1^{min}} = \frac{\varphi_{d2} - 1}{U_2 - U_2^{min}} \tag{13}$$

This function may be described as the difference between the marginal benefits of BS1 and BS2 when device i_s is attached with them. Thus, we may identify whether a device should be connected to BS2 or BS1 by determining alike the function $f(\varphi_{d1}, \varphi_{d2})$ is smaller or larger than zero. The indices of devices are organized with fixed values of $U = (U_1 - U_1^{min})(U_2 - U_2^{min})$ to make $f(\varphi_{d1}, \varphi_{d2})$ decrease in i_s, such that $f(\varphi_{d1}, \varphi_{d2})$ is a monotonic function of d.

This two-band device partition algorithm has the complexity of $O(D^2)$ for each iteration. The binary search algorithm can further improve it with complexity $O(D \log_2 D)$ for each iteration. The simulation indicates that this two-band device division approach converges after three rounds.

Table 1. Two-band device partition for NBS based devices association

Step 1. $\boldsymbol{Initialization}$
- Initialize the device association, such that each BS minimal payoff can be guaranteed and set maximum utility at iteration ***it=0***.
- Calculate $\boldsymbol{U_{max}(0) = U(0)}$.
- Set it=1.
Step 2. $\boldsymbol{Sorting}$
- Arrange devices in descending order according to $\boldsymbol{f(\varphi_{d1}, \varphi_{d2})}$.
Step 3. $\boldsymbol{For\ d = 1, \ldots, D - 1}$
- Calculate $\boldsymbol{U(d)}$, where devices $\boldsymbol{1, \ldots, d}$ are attached with first BS and devices $\boldsymbol{d + 1, \ldots, D}$ is associated with the second BS.
$\boldsymbol{End\ For}$
Step 4. $\boldsymbol{Choose\ the\ two - band\ partition}$
- $\boldsymbol{\mathcal{F}}$ = arg $\max_{d} \boldsymbol{U}\ (\boldsymbol{d})(\boldsymbol{corresponding\ d})$.
- That generates the largest $\boldsymbol{U}$ satisfying the constraints.
- Set $\boldsymbol{U_{max}\ (it) = U(\mathcal{F})}$.
Step 5. $\boldsymbol{Update\ device\ association}$
- If $\boldsymbol{U_{max}\ (it - 1) \prec U_{max}\ (it)}$, set it = it + 1,
- update $\boldsymbol{(U_1 - U_1^{min})(U_2 - U_2^{min})}$ based on the new partition,
- and **go to step 2.**
- Otherwise, the iteration ends.

Table 2 describes the procedure of the Hungarian algorithm.

Table 2. The procedure of Hungarian algorithm

Step 1. ***Subtract*** the row minimum from the entries in each row of $\mathcal{Z}$ - each row has at least one zero.
Step 2. ***Subtract*** the column minimum from the entries in each column of $\mathcal{Z}$ - each row and each column have at least one zero.
Step 3. ***Select*** rows and columns, and draw line across them, - all zeros are covered, and the number of lines is minimum
Step 4. ***If the number of lines*** $= \mathcal{B}$ - the produce is done - select a combination from the modified matrix, and the sum of such combination is zero. ***If the number of lines*** $< \mathcal{B}$ - **go to step 5.**
Step 5. ***Find*** the smallest entry that is not covered by any line, - subtract it from each entry that is not covered by lines, - add it to each entry which is covered by lines, - **go to step 3.**

4.3 Scheme for Multi-BS case with coalition

When there are more than two BSs, most published work focuses on resolving the device connected issue across several BSs via a centralized mechanism. Due to the combinatorial nature of the problem, this centralized solution, such as brute force, would incur a high computing cost and complexity with $O(D^{\mathcal{B}})$, practically unachievable for even medium-sized HCNs. This letter proposes a two-step iterative method. To begin, BSs are classified into pairs known as coalitions. Then, the two-player bargaining mechanism described in Table 1 is applied to each coalition. The BSs are reorganized and renegotiated until convergence occurs. This reduces the computational complexity significantly. Creating pairs of BSs is an assignment issue. BSs are often randomly paired to bargain the device association, which is the most frequent approach to solving this issue. A slower convergence rate may be expected if speed is gauged by the number of rounds of bargaining since there will be minimal benefit from negotiating in the randomly grouped pair. An assignment issue may be solved using the Hungarian method [43, 44] to minimize computational complexity and speed up convergence. Details of this assignment difficulty will be modelled as below. First, we specify the interest for nth BS to bargain with $\mathcal{K}th$ BS as $\mathcal{Z}_{n\mathcal{K}}$, which is theorized as an element of the matrix $\mathcal{Z}$. Where $\breve{U}_n$, $\breve{U}_{\mathcal{K}}$ represents the payoff for BS n and BS $\mathcal{K}$ if bargaining occurs, and $\widehat{U}_n$, $\widehat{U}_{\mathcal{K}}$ represents the payoff for BS n and BS $\mathcal{K}$ before bargaining. Without a doubt, $\boldsymbol{z}$ is symmetric, and $\mathcal{Z}_{nn}$ = 0, $\forall n$. The technique in Table 1 for partitioning two-band devices is utilized to identify each $\mathcal{Z}_{n\mathcal{K}} \forall n,\mathcal{K}$. The computational complexity is about $O(\mathcal{B}^2 D \log_2 D)$.

The coalition assignment matrix ω = $[\mathcal{Z}_{n\mathcal{K}}]$ with each element is defined as

$$\mathcal{Z}_{n\mathcal{K}} = \max_{n,\mathcal{K} \in \mathcal{B}} \left(U(\breve{U}_n, \breve{U}_{\mathcal{K}}) - U(\widehat{U}_n, \widehat{U}_{\mathcal{K}})\right) \tag{14}$$

$$\omega_{n\mathcal{K}} = \begin{cases} 1, \text{if BS } n \text{ bargains with BS } \mathcal{K} \\ 0, \qquad \text{otherwise} \end{cases} \tag{15}$$

As result, the assignment problem is phrasing the bargaining pair to maximize the overall performance, stated in (16).

$$\max_{\omega} \sum_{n\in\mathcal{B}} \sum_{k\in\mathcal{B}} \omega_{n\mathcal{K}}\, \mathcal{Z}_{n\mathcal{K}} \tag{16}$$

$$S.t. \qquad \textstyle\sum_{n\in B} \omega_{n\mathcal{K}} = 1, \ \forall\, \mathcal{K} \in \mathcal{B} \tag{16a}$$

$$\sum_{k\in B} \omega_{nk} = 1, \quad \forall \mathcal{K} \in \mathcal{B} \tag{16b}$$

$$\omega_{n\mathcal{K}} \in \{0,1\}, \quad \forall\, n, \mathcal{K} \in \mathcal{B} \tag{16c}$$

Since the Hungarian algorithm's minimization objective is the overall cost, the optimization objective orientation of (16) may be reformulated to $\max_{\omega} \sum_{n\in\mathcal{B}} \sum_{k\in\mathcal{B}} -\omega_{n\mathcal{K}}\, \mathcal{Z}_{n\mathcal{K}}$.

Table 3 displays the NBS-based device association method for multiple BS.

Table 3. NBS based device association algorithm for multi-BS

Step 1. ***Initialization the device association*** - Associate all devices, eMBBDs and uRLLCDs, to BSs.
Step 2. ***Coalition grouping*** - If the number of players is odd, a dummy BS is added to make the number of BSs even, and no BS bargains devices with this dummy BS. - Random Method: Group the 2-BS coalition randomly. - Hungarian Algorithm: The coalition is grouped by the algorithm in **Table 2.**
Step 3. ***Bargain within each coalition*** - Negotiate between two players in all coalitions using two-band devices partitions in **Table 1 (starting from step 2).**
Step 4. ***Repeat*** - Go back to step 2 until no further improvement is observed, i.e., $\mathcal{Z} = \mathbf{0}_{\mathcal{B}\times\mathcal{B}}$.

5. PROPOSED DAA BASED DEVICES PAIRING

Each BS restricts the wireless bandwidth and number of RBs. In a coexistence situation between uRLLC and eMBB, the objective of the BS is to satisfy the uRLLC QoS criteria and increase the QoS of eMBB customers serviced. This may be accomplished by superimposing the uRLLC users on the current eMBB connection in an effective manner. Consequently, each BS needs an incentive mechanism to encourage uRLLC users to apply superposition. To encourage uRLLC users for superposition, we employ the H-NOMA matching theory framework, and each BS constructs a bundle of contracts for uRLLC users. By superimposing the current eMBB transmissions, we propose that eMBB traffic be sent through long TTIs T, whilst uRLLC load is broadcast through short TTIs; thus, the transmitting incoming uRLLC traffic guarantees its delay demand. Using Figure 2's instructive example, we may have a deeper understanding of the problem's underlying philosophy and the proposed solution. After the association process, each BS has adequate traffic for linked eMBBDs and uRLLCDs. Thus, eMBBDs are scheduled on all accessible RBs at the beginning of a time slot and remain fixed for the duration of the slot. Let's suppose that, at the

beginning of the time slot, each related eMBBD with BS b has n RBs per long TTI based on achieving justice in section 4 between the devices. In general, the uRLLC load has a little packet size and also suffers from the tough delay bindings of its load; thus, it demands a portion of whole mini-slots for its load. We seek to ensure the least delay and the highest reliability of uRLLCDs, so we choose the H-NOMA technique to utilize for the uRLLC traffic in this research. When uRLLC traffic is received to BS attached with it (in any mini-slot of the instant time slot), a BS attempts to superimposition a uRLLCD with an appropriate eMBBD under avhieving all limitations both of slices and devices through mini-slot m, as shown in Figure 2. And the scheduler aims at immediately scheduling such traffic with ρ_{le} paired mini-slots. Keeping the problem's (17) purpose in mind, the issue is how to choose the appropriate eMBBD, and the number of coupled mini-slots that the eMBBD presently allocates are the best to be superimposed. Therefore, a BS equalizes the rate of eMBBDs in every long TTI, in the end optimizing the target of (17) on a long-term.

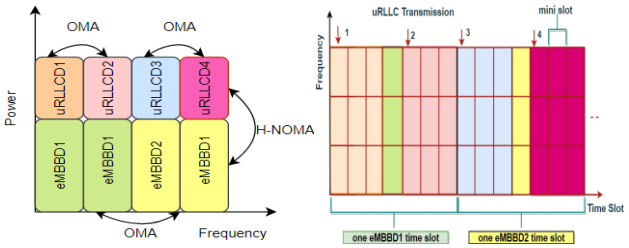

Figure 2. Illustration of the proposed H-NOMA for eMBBDs and uRLLCDs

5.1 Problem formulation

After the device association process is done, to complete our target by maximizing the network's total throughput. Besides let $\mathcal{X} \in \{0, 1\}$, denote the matrix of pairing by H-NOMA technique at the same BS b, where x_{le}^{nm}= 1 if l the device is paired with $e$device by superposition scheme,0 otherwise. The DL rate is an indispensable standard for these devices utilizing the superposition technique between eMBBDs and uRLLCDs based on H-NOMA, keeping the same objective of (10) with fixed a^t, $\forall\, \mathcal{T}$ are shown as follows:

$$\text{O. P. T2} - \text{DP: } \max_{\{x\}} \ [F_1(x)]^T \tag{17}$$

$$\text{S.t. } x_{le}^{nm} \in \{0,1\},\ \forall\, m \in M, n \in \mathcal{N},\ b \in \mathcal{B} \tag{17a}$$

$$\sum_{e \in D^{eMBB}} x_{le}^{nm}\, R_{be} \le \mathcal{R}_1^{rsv} \qquad \forall\, m \in M, b \in \mathcal{B} \tag{17b}$$

$$\sum_{l \in D^{uRLLC}} x_{le}^{nm}\, R_{bl} \le \mathcal{R}_1^{rsv} \qquad \forall\, m \in M, b \in \mathcal{B} \tag{17c}$$

where, $F(a) = \sum_{b \in \mathcal{B}} \sum_{e \in D^{eMBB}} R_{be} + \sum_{b \in \mathcal{B}} \sum_{l \in D^{uRLLC}} R_{bl}$, is the total rate for eMBBDs and uRLLCDs. Condition (16a) implies that the pairing indicators are binary values. Condition (15b) and (15c) achieve the inter-slice interference isolation among slices' uRLLC and eMBB per each $\mathcal{B}$ and guarantee the QoS for every slice based on H-NOMA technique.

5.2 Matching game based DP algorithm

The capability of the matching game to solve combinatorial issues is what makes it a good choice for the device pairing problem. The major the matching theory merits are [45]: 1) The factual enforcements enable a self-organizing, widely dispensed, and low-data-exchange solution to the DP problem, which is basically necessary for critical-processing devices (uRLLCDs). 2) It is a powerful tool that can be used to analyze interactions between a large number of players with a large number of possible strategies. 3) The power to determine unique utilities for various players with distinct needs (such as eMBBDs and uRLLCDs) based on their limited data. Consequently, a matching game is proper to be utilized for the DP problem as (17). In this subsection, we apply matching algorithm to solve the DP subproblem is formulated as a one-to-one matching theory. The matching role of DP is specified by Λ_{DP} with a tuple $\left(D^{uRLLC}, D^{eMBB}, \tilde{\Theta}, \succ_{D^{uRLLC}}, \succ_{D^{eMBB}}\right)$. In the DP matching function, $\succ_{D^{uRLLC}} = \{\succ_l\}_{l \in D^{uRLLC}}$ and $\succ_{D^{eMBB}} = \{\succ_e\}_{e \in D^{eMBB}}$ indicate the preference relevances of the connected uRLLCDs and the eMBBDs with BS b, respectively. We suppose that $\tilde{\Theta}$ is the quota for O.P.T2- DP. Definition 1: Given two disjoint finite sets of players D^{uRLLC} and D^{eMBB}, such that 1) $|\Lambda_{\text{DP}}(e)| \le \widetilde{\Theta_e}$ and $\Lambda_{\text{DP}}(e) \in D^{uRLLC}$, $e \in D^{eMBB}$, where $\widetilde{\Theta_e}$ is the quota of e and $\widetilde{\Theta_e} = Q$ per TTI. 2) $|\Lambda_{\text{DP}}(l)| \le \widetilde{\Theta_l}$ and $\Lambda_{\text{DP}}(l) \in D^{eMBB}$, $l \in D^{uRLLC}$, where $\widetilde{\Theta_l}$ is the quota of l and $\widetilde{\Theta_l} = 1$. 3) $e \in \Lambda_{\text{DP}}(l) \leftrightarrow l \in \Lambda_{\text{DP}}(e)$. The DP pairing mapping is the result of the matching game. In the superimposing scenario of eMBB and uRLLC, each uRLLCD can pair with only one eMBBD per mini-slot m, but eMBBD might be coupled with an extreme of $\tilde{\Theta}$ uRLLCDs per time slot t. Whereas, we suppose the time slot t as Q sub-time slots and use a one-to-one matching game between uRLLC and eMBB slices each sub-time slot. As for O.P.T2- DP, we erect the preference lists of eMBBDs and uRLLCDs based on the following utility functions as $\psi_e(l)$ and $\psi_l(e)$.

- **eMBBDs Utility Function**

First, each eMBBD ranks its paired uRLLCD with the lowest rate to possess the complete RB without a partner. The preference utility of each eMBBD will then be as follows:

$$\psi_e(l) = R_{bl} \tag{18}$$

- **uRLLCDs Utility Function**

In order to achieve uRLLC latency and reliability constraints, each uRLLCD ranks the associated eMBBDs in the same BS with the greatest rate. The preference utility of each uRLLCD is based on the following preferences:

$$\psi_l(e) = R_{be} \tag{19}$$

The main details of the DP algorithm are described in Algorithm. After initialization, for each BS, sort eMBBDs in descending order to construct the preference relations for uRLLCDs $H_l \succ_l$ using (19) at each iteration It. Similarly, the preference list for each eMBBD H_e is which is constructed dependent on the preference utility (18) (step 6-9). Assign the quota of each eMBBD per time slot. Each eMBBD is unpaired send the request to their preferred uRLLCDs (step 10). Each uRLLCD will then decide to accept the requests or not, dependent on its defined utility, its quota $\tilde{\Theta}_l^{rem}$ and threshold rate for each slice's BS. If uRLLCD l has sufficient $\tilde{\Theta}_l^{rem}$ to e, it agrees and modifies the requests $\tilde{\Theta}_l^{rem}, \tilde{\Theta}_e^{rem}$ and $\Lambda_{DP}^{(It)}(l)$ (step 15-17). Otherwise, if the quota of l is not sufficient, but

the utility (19) of the requesting device e is larger than that of $\hat{e}$ it accepted in the previous round, the uRLLCD l determines its current matched $\hat{e}$ which have a worse ranking than e according to H_l^{It} (steps 18-20). Each least preferred $\hat{e}$ is then sequentially removed and $\tilde{\Theta}_{\hat{e}}^{rem}$, $\tilde{\Theta}_e^{rem}$, the minimum preference list (ξ_{mp}) and $\Lambda_{DP}^{(It)}(l)$ are updated and e_b can be admitted or there is no $\hat{e}$ to refuse (steps 21-28). After many repetitions of t, there are no trialling uRLLCDs; then, the algorithm achieves to a stable matching. The main goal of the presented matching game is to achieve stable matching. So, we demand to locate the blocking couple for the match, let us indicate through: $\Lambda_{\mathrm{DP}}(l, e)$ the subset of all possible matchings between D^{uLLC} and D^{eMBB}. Thus, the game is stable if there no blocking couple occurs. A pair $(l, e) \neq \Lambda_{\mathrm{DP}}$, where $l \in D^{uRLLC}$, $e \in D^{eMBB}$ is became to be a blocking pair for the matching Λ_DP if it is not blocked by a unique device e and device l, and there is another matching $\Lambda_{\mathrm{DP}}{}' \in \Lambda_{\mathrm{DP}}(l, e)$ such as device e and device l, can attain a higher utility. Hence, given fixed preference relations of eMBBDs and uRLLCDs, the matching game algorithm is known as the deferred acceptance algorithm (DAA) [27] in two-sided matching, which converges to a stable match. Note that, the worst-case computational complexity of DP algorithm is linear in the size of its preference lists, i.e., $O(D^{eMBB} D^{uRLLC})$.

Algorithm: Matching game for device pairing

Input: $D^{eMBB}, D^{uRLLC}, \mathcal{B}$

Output: Find stable Matching $\Lambda_{DP}^{(It)}$

Initialization, $It = 0, \Lambda_{DP}^{(It)} = \left\{\Lambda_{DP}^{(It)}(l), \Lambda_{DP}^{(It)}(e)\right\}_{l \in D^{uRLLC}, e \in D^{eMBB}, b \in \mathcal{B}} = \emptyset,$
$\xi_{mp} = \emptyset, \tilde{\Theta}_l = \left\{\tilde{\Theta}_l^{rem} = 0, \tilde{\Theta}_e^{rem} = 0, \tilde{\Theta}_e^{mod} = 0\right\}_{e \in E, l \in \mathcal{L}, b \in \mathcal{B}}$

Repeat
  $It \leftarrow It + 1$
  for $b \in \mathcal{B}$ **do**
    Sorts D^{eMBB} allocated with b in descending order dependent on the achievable rate
    for $e \in D^{eMBB}$ sort **do**
      $H_e^{It} \leftarrow$ BS b construct $\succ_e$ using $\psi_e(l)$
      $\tilde{\Theta}_e^{rem} \leftarrow \mathcal{L}/E$
      $\tilde{\Theta}_e^{mod} \leftarrow |\mathcal{L}| \bmod |E|$
      If $\tilde{\Theta}_e^{mod} > 0$ **do**
        $\tilde{\Theta}_e^{rem} \leftarrow \tilde{\Theta}_e^{rem} + 1$
      while $e \notin \Lambda_{DP}^{(It)}(l)$ and $H_e^{It} \neq \emptyset$ **do**
        If $\Theta_l^{rem} = 0$ **then**
          $\Lambda_{DP}^{(It)}(l) \leftarrow \Lambda_{DP}^{(It)}(l) \cup \{e\},$
          $\tilde{\Theta}_e^{rem} \leftarrow \tilde{\Theta}_e^{rem} - 1,$
          $\Theta_l^{rem} \leftarrow \Theta_l^{rem} + 1$
        else
          $\hat{H}_l^{It} \leftarrow \left\{\hat{e} \in \Lambda_{DP}^{(It)}(e) | e \succ_l \hat{e}\right\},$
          $\xi_{mp} \leftarrow \hat{e} \in \hat{H}_l^{It}$
          while $\hat{H}_l^{It} \cup (\tilde{\Theta}_l^{rem} = 1)$ **do**
            $\Lambda_{DP}^{(It)}(l) \leftarrow \Lambda_{DP}^{(It)}(l) \backslash \{\xi_{mp}\},$
            $\hat{H}_l^{It} \leftarrow \hat{H}_l^{It} \backslash \{\xi_{mp}\},$
            $\Theta_{\hat{e}}^{rem} \leftarrow \Theta_{\hat{e}}^{rem} + 1$
            $\xi_{mp} \leftarrow \hat{e} \in \hat{H}_l^{It}$
            $\Lambda_{DP}^{(It)}(l) \leftarrow \Lambda_{DP}^{(It)}(l) \cup \{e\},$
            $\tilde{\Theta}_e^{rem} \leftarrow \tilde{\Theta}_e^{rem} - 1$
until $\Lambda_{DP}^{(It)}(l) = \Lambda_{DP}^{(It-1)}(l)$

6. NUMERICAL RESULTS

We consider a two-tier HCN with one MBS and three PBSs. The number of eMBBDs and uRLLCDs are set to be 50 and 100, respectively. PBSs and devices are uniformly distributed within a 250-meter radius in the urban environment. The essential simulation parameters are shown in Table 4 [11, 46] as shown in Figure 3. The simulations are based 500 times to assure accuracy and average results.

To demonstrate how well the proposed technique works for handling diverse device classes with the device association and pairing metrics, its performance is compared with that of other existing schemes like the Max-SINR scheme and greedy heuristic algorithm (GHA, GA) in different techniques (H-NOMA, Puncturing and OMA). Because of the multiuser diversity advantage, the overall rate grows as the number of devices increases.

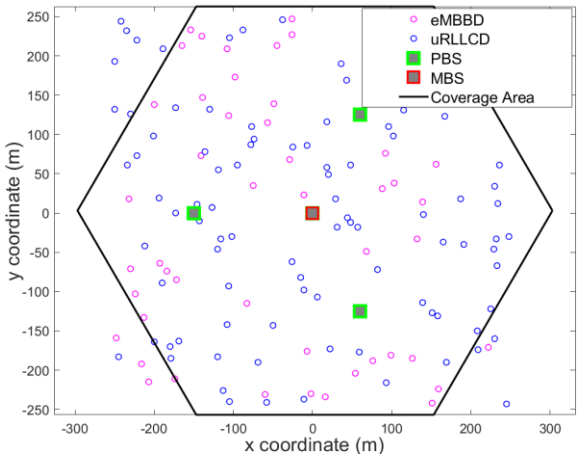

Figure 3. A snapshot of the simulated network situation scenario, with the MBS in the cell's centre, three PBSs along with the MBS, and devices randomly spread across the HCN's geographical region

Table 4. Simulation parameters

Parameter	Value	Parameter	Value
5G RAN bandwidth	20MHz	Inter-site distance	500m
RB bandwidth	180kHz	Modulation	64QAM
Number of RBs	100	Log-normal shadowing	10 dB
Transmit power of MBS	46dBm	eMBB rate threshold	[1-4] Mbps
Transmit power of PBS	3dBm	uRLLC rate threshold	[0.1-1.6] Mbps
Noise power	$174\frac{dB_m}{Hz}$	uRLLC packet size	[32-256] bytes
PHY numerology	15 kHz subcarrier spacing;12 subcarriers per RB; 2-OFDM symbols TTI (0.143 msec)		
HARQ	Asynchronous HARQ with chase combining, and 4 TTI round trip time; Max 6 HARQ retransmissions.		

*d is the distance in Km between device and MBS or PBS

Figures 4 and 5 provide a comparison of the cumulative distributions of the DL devices' rate for the proposed system and compared works. The recommended correlation technique beats all other approaches, demonstrating its use in this graph. Because our proposed method considers the device's

requirements, it seeks to link eMBBDs with BS and uRLLCDs at a low rate in order to maximise the DL data rate for all devices. However, in all presented schemes, the proposed strategy outperformed alternative techniques using the same power allocation mechanism. In addition, the overall sum rate for OMA is less than that for NOMA, demonstrating that H-NOMA is extra overall-rate effective than OMA. In addition, the NOMA algorithm presented is superior to the Puncturing method proposed. As for OMA, although we assume that it gains 1/2 power of a RB, only a portion of the RBs is exploited based on our assumption 25% based on [47]; as for H-NOMA, it is available to all RBs' BS; additionally, PUNC, when overlapping uRLLCD, it takes away one mini-slot with all allocated eMBBD's RBs Consequently, our presumptive architecture delivers the highest DL data rate for both devices.

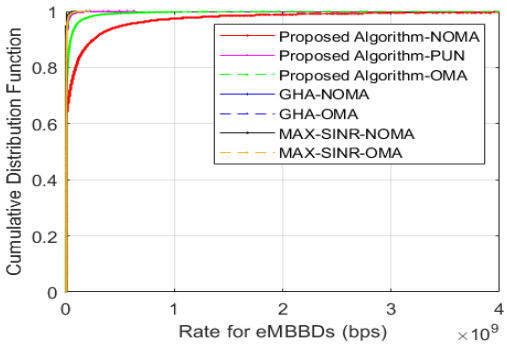

Figure 4. CDF of rate for eMBBDs in HCNs

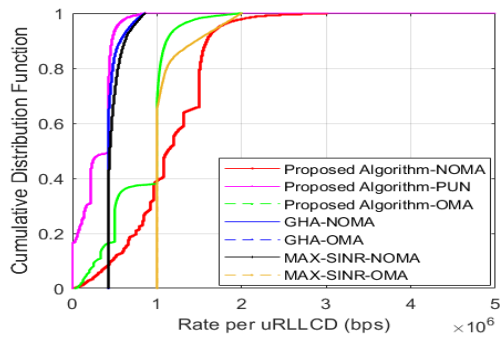

Figure 5. CDF of rate for uRLLCDs in HCNs

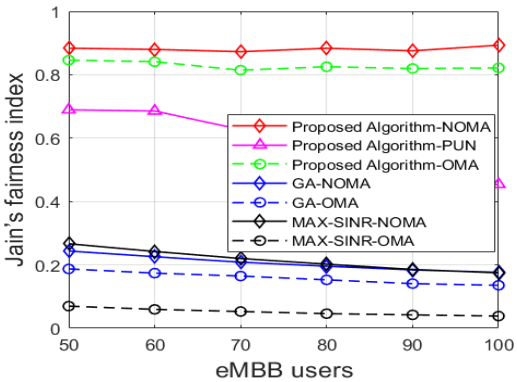

Figure 6. Jain's fairness index for eMBBDs

To validate fairness performance among devices in different association schemes, Jain Index (JI) is one of the quantitative as well as notable measures to evaluate fairness and is defined as follows: $J = \frac{(\sum_{i\epsilon\mathcal{D}} x_i)^2}{\mathcal{D} \sum_{i\epsilon\mathcal{D}} {x_i}^2}$, x_i is the measurement metric, $\mathcal{D}$ is number of devices. To esteem fairness amongst eMBBDs, we set $x_i = r_i$, $i = 1,2, \dots, D^{eMBB}$ and $\mathcal{D} = D^{eMBB}$, r_i is the DL transmission rate for eMBBD. Also, to achieve fairness between uRLLCDs, we put $x_i = {r_i}^m$, $i = 1,2, \dots, D^{uRLLC}$ and $\mathcal{D} = D^{uRLLC}$, ${r_i}^m$ is the DL transmission rate for uRLLCD. Figure 6 shows the fairness of eMBBDs as the number of eMBBDs grows from 50 to 100, and the number of uRLLCDs equals 100. Meanwhile, Figure 7 displays the fairness among uRLLCDs when the number of uRLLCDs grows from 50 to 100 and the number of eMBBDs equals 50. Figures 6 and 7 depict Jain's fairness index for the proposed method and comparable algorithms. As can be observed, the suggested method beats the competing algorithms regarding device fairness. This verifies that each device has made an adaptive decision to promote equality among devices.

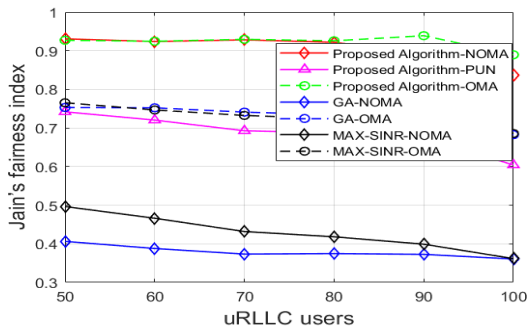

Figure 7. Jain's fairness index for uRLLCDs

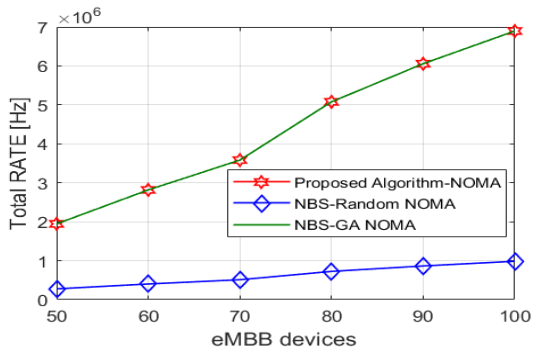

Figure 8. The total Rate for eMBBDs against number of eMBBDs

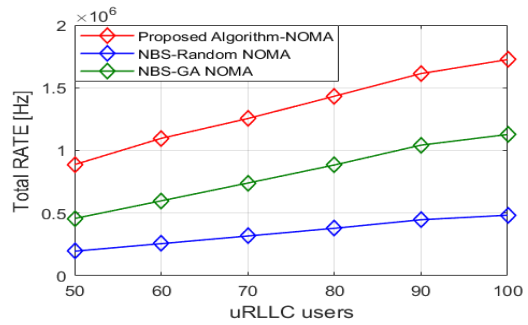

Figure 9. The total Rate for uRLLCDs against number of uRLLCDs

Figure 8 illustrates the overall rate of eMBBDs with various numbers of eMBBDs by applying the scenario with 100 uLLCDs. The overall rate of eMBBDs across all schemes grows as the number of eMBBDs increases. eMBB devices interest more in the DL data rate. During the device connection

and coupling procedures, the throughput is provided to eMBBDs based on the BS connected with them and the number of resource blocks allocated via NBS; regardless of the pairing techniques like a matching game and a greedy algorithm, the two shapes are similar. In comparison, the performance of the proposed H-NOMA algorithm remains superior to the Random-NOMA technique; thus, the suggested algorithm achieves a better DL overall rate for eMBBDs by 60% than Random H-NOMA. Figure 9 shows the total throughput for uRLLCDs when the number of uRLLCDs goes between 50 and 100 and the number of eMBBDs stays at 50. It is clear that the overall sum rate for uRLLCDs goes up as the number of uRLLCDs goes up. Further, the proposed correlation's execution strategy on the matching game does better than all the other schemes. It proves how efficiently the proposed pairing approaches work due it takes into account the type of device, its requirements, and the isolation constraints between devices. Compared to "GA-NOMA" and "Random-NOMA" schemes, the proposed simulation results show potential better gains of rate optimization for uLLC load with its pairing based on the matching game approach by 10% and 37%, respectively. Figure 10 displays the DL delay for uRLLC while its DL packet size grows for uRLLCD. Figure 10 confirms that the suggested approach proceeds preferably than other algorithms. Based on the transmission time, our proposed method shows that every uRLLC packet can be transmitted in lower than 1 ms, whether it is attached with MBS or PBS. Applying the scenario with 50 eMBBDs and 100 uLLCDs as a model, compared with "Random H-NOMA" and "greedy H-NOMA" algorithms, the proposed algorithm provides for uRLLC delay traffic up to 22% and 25%, respectively.

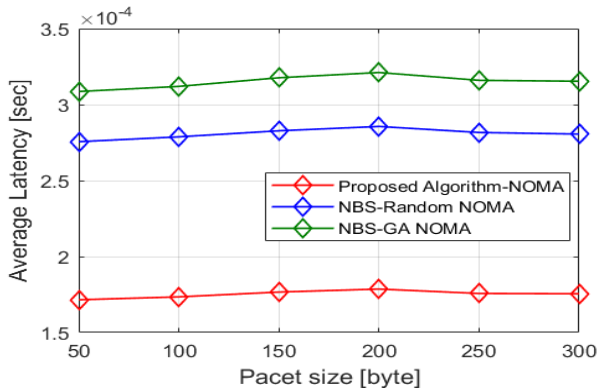

Figure 10. The mean delay against uRLLC offered packet

7. CONCLUSIONS

This essay suggests a fair device association scheme for pairing multi-service eMBB and uRL LC in HCN. Whereas the device association problem is set up as a cooperative Nash bargaining game that deems the different needs for eMBBDs and uRLLCDs to ensure all devices are treated fairly and get the most use out of them. While the pairing process is set up as a multi-objective combinatorial optimization problem to maximise the total DL rate for eMBBDs and subject to uRLLC latency and reliability constraints, it is dependent on a matching theory; also, the interference between slices has been limited by using flexible rate isolation. It was shown that the submitted solution was better than the throughput-oriented approach in terms of how well it worked and improved a big rate benefit (37% vs. Random H-NOMA scheme) and (10% greedy H-NOMA algorithm [2]) for uRLLCDs. Also, the submitted strategy provides a worthy rate gain of 60% compared with the Random H-NOMA scheme. uRLLC-eMBB slicing is used in delay-sensitive applications such as self-driving and Support VR Virtual reality (VR) [48].

In future work, we will endeavour NOMA-slicing with a hybrid overlay-underlay spectrum access platform in HCNs to provide energy efficacy to minimise CCI. Also, we may study a DL underlay cognitive radio-NOMA (CR-NOMA) in HCN to decrease CCI and improve the execution of spectrum participating. We can gather HCNs with aerially controlled networks like Unmanned Aerial Vehicles (UAVs) are needed to defeat most of the defiances [49, 50].

REFERENCES

[1] Parkvall, S., Dahlman, E., Furuskar, A., Frenne, M. (2017). NR: The new 5G radio access technology. IEEE Communications Standards Magazine, 1(4): 24-30. https://doi.org/10.1109/MCOMSTD.2017.1700042

[2] Pepper, R. (2013). Cisco visual networking index (VNI) global mobile data traffic forecast update. Technical Report, Cisco.

[3] Liu, D.T., Wang, L.F., Chen, Y., Elkashlan, M., Wong, K. K., Schober, R., Hanzo, L. (2016). User association in 5G networks: A survey and an outlook. IEEE Communications Surveys & Tutorials, 18(2): 1018-1044. https://doi.org/10.1109/COMST.2016.2516538

[4] Islam, S.M.R., Avazov, N., Dobre, O.A., Kwak, K.S. (2016). Power-domain non-orthogonal multiple access (NOMA) in 5G systems: Potentials and challenges. IEEE Communications Surveys & Tutorials, 19(2): 721-742. https://doi.org/10.1109/COMST.2016.2621116

[5] Zhang, X.C., Haenggi, M. (2014). The performance of successive interference cancellation in random wireless networks. IEEE Transactions on Information Theory, 60(10): 6368-6388. https://doi.org/10.1109/TIT.2014.2341248

[6] Series, M. (2017). Minimum requirements related to technical performance for IMT-2020 radio interface (s). Report M. 2410, ITUWRC.

[7] Popovski, P., Stefanović, Č., Nielsen, J.J., De Carvalho, E., Angjelichinoski, M., Trillingsgaard, K.F., Bana, A.S. (2019). Wireless access in ultra-reliable low-latency communication (URLLC). IEEE Transactions on Communications, 67(8): 5783-5801. https://doi.org/10.1109/TCOMM.2019.2914652

[8] Elayoubi, S.E., Jemaa, S.B., Altman, Z., Galindo-Serrano, A. (2019). 5G RAN slicing for verticals: Enablers and challenges. IEEE Communications Magazine, 57(1): 28-34. https://doi.org/10.1109/MCOM.2018.1701319

[9] Kazmi, S.M. A., Khan, L.U., Tran, N.H., Hong, C.S. (2019). Network slicing for 5G and beyond networks. Springer Cham. https://doi.org/10.1007/978-3-030-16170-5

[10] Riggio, R., Bradai, A., Harutyunyan, D., Rasheed, T., Ahmed, T. (2016). Scheduling wireless virtual networks functions. IEEE Transactions on Network and Service Management, 13(2): 240-252. https://doi.org/10.1109/TNSM.2016.2549563

[11] Guo, T., Suárez, A. (2019). Enabling 5G RAN slicing

with EDF slice scheduling. IEEE Transactions on Vehicular Technology, 68(3): 2865-2877. https://doi.org/10.1109/TVT.2019.2894695

[12] Popovski, P., Trillingsgaard, K.F., Simeone, O., Durisi, G. (2018). 5G wireless network slicing for eMBB, URLLC, and mMTC: A communication-theoretic view. IEEE Access, 6: 55765-55779. https://doi.org/10.1109/ACCESS.2018.2872781

[13] Ding, Z.G., Lei, X.F., Karagiannidis, G.K., Schober, R., Yuan, J.H., Bhargava, V.K. (2017). A survey on non-orthogonal multiple access for 5G networks: Research challenges and future trends. IEEE Journal on Selected Areas in Communications, 35(10): 2181-2195. https://doi.org/10.1109/JSAC.2017.2725519

[14] Dos Santos, E.J., Souza, R.D., Rebelatto, J.L. (2021). Rate-splitting multiple access for URLLC uplink in physical layer network slicing with eMBB. IEEE Access, 9: 163178-163187. http://dx.doi.org/10.1109/ACCESS.2021.3134207

[15] Chen, Q., Wang, J., Jiang, H. (2021). URLLC and eMBB coexistence in MIMO non-orthogonal multiple access systems. arXiv preprint arXiv:2109.05725. https://doi.org/10.48550/arXiv.2109.05725

[16] Almekhlafi, M., Arfaoui, M.A., Elhattab, M., Assi, C., Ghrayeb, A. (2021). Joint resource allocation and phase shift optimization for RIS-aided eMBB/URLLC traffic multiplexing. IEEE Transactions on Communications, 70(2): 1304-1319. https://doi.org/10.1109/TCOMM.2021.3127265

[17] Esswie, A.A., Pedersen, K.I. (2018). Opportunistic spatial preemptive scheduling for URLLC and eMBB coexistence in multi-user 5G networks. IEEE Access, 6: 38451-38463. https://doi.org/10.1109/ACCESS.2018.2854292

[18] Matera, A., Kassab, R., Simeone, O., Spagnolini, U. (2018). Non-orthogonal eMBB-URLLC radio access for cloud radio access networks with analog fronthauling. Entropy, 20(9): 661. https://doi.org/10.3390/e20090661

[19] Alsenwi, M., Tran, N.H., Bennis, M., Bairagi, A.K., Hong, C.S. (2019). eMBB-URLLC resource slicing: A risk-sensitive approach. IEEE Communications Letters, 23(4): 740-743. https://doi.org/10.1109/LCOMM.2019.2900044

[20] Alsenwi, M., Tran, N.H., Bennis, M., Pandey, S.R., Bairagi, A.K., Hong, C.S. (2021). Intelligent resource slicing for eMBB and URLLC coexistence in 5G and beyond: A deep reinforcement learning based approach. IEEE Transactions on Wireless Communications, 20(7): 4585-4600. https://doi.org/10.1109/TWC.2021.3060514

[21] Anand, A., De Veciana, G., Shakkottai, S. (2020). Joint scheduling of URLLC and eMBB traffic in 5G wireless networks. IEEE/ACM Transactions on Networking, 28(2): 477-490. https://doi.org/10.1109/TNET.2020.2968373

[22] Gu, Y., Saad, W., Bennis, M., Debbah, M., Han, Z. (2015). Matching theory for future wireless networks: Fundamentals and applications. IEEE Communications Magazine, 53(5): 52-59. https://doi.org/10.1109/MCOM.2015.7105641

[23] Le, T.H.T., Tran, N.H., LeAnh, T., Hong, C.S. (2016). User matching game in virtualized 5G cellular networks. In 2016 18th Asia-Pacific Network Operations and Management Symposium (APNOMS), pp. 1-4, IEEE. https://doi.org/10.1109/APNOMS.2016.7737278

[24] Manzoor, A., Kazmi, S.M.A., Pandey, S.R., Hong, C.S. (2020). Contract-based scheduling of URLLC packets in incumbent EMBB traffic. IEEE Access, 8: 167516-167526. https://doi.org/10.1109/ACCESS.2020.3023128

[25] Elhattab, M.K., Elmesalawy, M.M., Salem, F.M., Ibrahim, I.I. (2019). Device-aware cell association in heterogeneous cellular networks: A matching game approach. IEEE Transactions on Green Communications and Networking, 3(1): 57-66. https://doi.org/10.1109/TGCN.2018.2881242

[26] Bairagi, A.K., Munir, M.S., Alsenwi, M., Tran, N.H., Alshamrani, S.S., Masud, M., Han, Z, Hong, C.S. (2020). Coexistence mechanism between eMBB and uRLLC in 5G wireless networks. IEEE Transactions on Communications, 69(3): 1736-1749. https://doi.org/10.1109/TCOMM.2020.3040307

[27] Liang, W., Ding, Z., Li, Y.H., Song, L.Y. (2017). User pairing for downlink non-orthogonal multiple access networks using matching algorithm. IEEE Transactions on communications, 65(12): 5319-5332. https://doi.org/10.1109/TCOMM.2017.2744640

[28] Tebe, P.I., Ntiamoah-Sarpong, K., Tian, W.H., Li, J., Huang, Y.J., Wen, G.J. (2020). Using 5G network slicing and non-orthogonal multiple access to transmit medical data in a mobile hospital system. IEEE Access, 8: 189163-189178. https://doi.org/10.1109/ACCESS.2020.3031306

[29] Zhang, K.J., Xu, X.D., Zhang, J.X., Zhang, B.F., Tao, X.F., Zhang, Y.T. (2021). Dynamic multiconnectivity based joint scheduling of eMBB and uRLLC in 5G networks. IEEE Systems Journal, 15(1): 1333-1343. https://doi.org/10.1109/JSYST.2020.2977666

[30] Amine, M., Kobbane, A., Ben-Othman, J. (2020). New network slicing scheme for UE association solution in 5G ultra dense hetnets. In ICC 2020-2020 IEEE International Conference on Communications (ICC), pp. 1-6, IEEE. https://doi.org/10.1109/ICC40277.2020.9148844

[31] Ma, M.Y., Wong, V.W.S. (2020). Joint user pairing and association for multicell NOMA: A pointer network-based approach. In 2020 IEEE International Conference on Communications Workshops (ICC Workshops), pp. 1-6. IEEE. https://doi.org/10.1109/ICCWorkshops49005.2020.9145383

[32] Dos Santos, E.J., Souza, R.D., Rebelatto, J.L., Alves, H. (2020). Network slicing for URLLC and eMBB with max-matching diversity channel allocation. IEEE Communications Letters, 24(3): 658-661. https://doi.org/10.1109/LCOMM.2019.2959335

[33] Liu, D.T., Chen, Y., Chai, K.K., Zhang, T.K., Elkashlan, M. (2014). Opportunistic user association for multi-service HetNets using Nash bargaining solution. IEEE Communications Letters, 18(3): 463-466. https://doi.org/10.1109/LCOMM.2014.012314.140090

[34] Parsaeefard, S., Dawadi, R., Derakhshani, M., Le-Ngoc, T. (2016). Joint user-association and resource-allocation in virtualized wireless networks. IEEE Access, 4: 2738-2750. https://doi.org/10.1109/ACCESS.2016.2560218

[35] Rezvani, S., Yamchi, N.M., Javan, M.R., Jorswieck, E.A. (2021). Resource allocation in virtualized CoMP-NOMA HetNets: Multi-connectivity for joint transmission. IEEE Transactions on Communications, 69(6): 4172-4185. https://doi.org/10.1109/TCOMM.2021.3067700

[36] Poornima, P., Laxminarayana, G., Rao, D.S. (2017). Performance analysis of channel capacity and throughput of LTE downlink system. International Journal of Computer Networks & Communications, 9(5): 55-69. http://dx.doi.org/10.5121/ijcnc.2017.9505

[37] Han, Z., Ji, Z., Liu, K.J.R. (2005). Fair multiuser channel allocation for OFDMA networks using Nash bargaining solutions and coalitions. IEEE Transactions on Communications, 53(8): 1366-1376. https://doi.org/10.1109/TCOMM.2005.852826

[38] Liu, D.T., Chen, Y., Chai, K.K., Zhang, T.K. (2014). Nash bargaining solution-based user association optimization in HetNets. In 2014 IEEE 11th Consumer Communications and Networking Conference (CCNC), pp. 587-592, IEEE. https://doi.org/10.1109/CCNC.2014.6866631

[39] Elhattab, M.K., Elmesalawy, M.M., Ibrahim, I.I. (2017). A game theoretic framework for device association in heterogeneous cellular networks with H2H/IoT co-existence. IEEE Communications Letters, 21(2): 362-365. https://doi.org/10.1109/LCOMM.2016.2620468

[40] Zhou, T.Q., Huang, Y.M., Yang, L.X. (2015). User association with jointly maximising downlink sum rate and minimising uplink sum power for heterogeneous cellular networks. IET Communications, 9(2): 300-308. https://doi.org/10.1049/iet-com.2014.0476

[41] Yu, W., Cioffi, J.M. (2000). FDMA capacity of gaussian multiple-access channels with ISI. IEEE International Conference on Communications, 50(1): 102-111. https://doi.org/10.1109/ICC.2000.853720

[42] Sadeghi, E., Behroozi, H., Rini, S. (2020). Fairness-oriented user association in hetnets using bargaining game theory. arXiv preprint arXiv:2011.04801.

[43] Papadimitriou, C.H., Steiglitz, K. (1982). Combinatorial optimization: Algorithms and complexity. IEEE Transactions on Acoustics Speech and Signal Processing. http://dx.doi.org/10.1109/TASSP.1984.1164450

[44] Kuhn, H.W. (2009). The Hungarian method for the assignment problem. In 50 Years of Integer Programming 1958-2008, Springer, 6: 29-47.

[45] Hasan, M., Hossain, E. (2017). Distributed resource allocation in 5G cellular networks. In: Vannithamby, R., Talwar, S., Towards 5G: Applications, Requirements and Candidate Technologies, 129-161. https://doi.org/10.1002/9781118979846.ch8

[46] Elsayed, M., Erol-Kantarci, M. (2019). AI-enabled radio resource allocation in 5G for URLLC and eMBB users. In 2019 IEEE 2nd 5G World Forum (5GWF), pp. 590-595, IEEE. https://doi.org/10.1109/5GWF.2019.8911618

[47] Ginige, N.U., Manosha, K.B.S., Rajatheva, N., Latva-aho, M. (2020). Admission control in 5G networks for the coexistence of eMBB-URLLC users. In 2020 IEEE 91st Vehicular Technology Conference (VTC2020-Spring), pp. 1-6, IEEE. https://doi.org/10.1109/VTC2020-Spring48590.2020.9129141

[48] Park, J., Bennis, M. (2018). URLLC-eMBB slicing to support VR multimodal perceptions over wireless cellular systems. In 2018 IEEE Global Communications Conference (GLOBECOM), pp. 1-7, IEEE. https://doi.org/10.1109/GLOCOM.2018.8647208

[49] Madan, H.T., Basarkod, P.I. (2020). Throughput and outage probability analysis for cognitive radio-non-orthogonal multiple access in uplink and downlink scenarios. Mathematical Modelling of Engineering Problems, 7(4): 659-666. https://doi.org/10.18280/mmep.070419

[50] Metwaly, S.S., Abd El-Haleem, A.M., El-Ghandour, O. (2020). NOMA based matching game algorithm for narrowband internet of things (NB-IoT) system. Ingénierie des Systèmes d'Information, 25(3): 345-350. https://doi.org/10.18280/isi.250308